J. Astrophys. Astr. (2006) **27,** 125–137

Physics of the Sun's Hot Atmosphere

B. N. Dwivedi
Department of Applied Physics, Institute of Technology, Banaras Hindu University, Varanasi 221 005, India.
e-mail: bholadwivedi@yahoo.com

Abstract. This article briefly overviews the physics of the Sun's hot atmosphere, using observations from recent solar spacecrafts: Yohkoh, SOHO, TRACE and RHESSI.

Key words. Solar atmosphere—X-ray and EUV emission—coronal heating—solar wind.

1. Introduction

The Sun has well-defined regions which can broadly be compared to the solid part of an Earth-like planet and its atmosphere (cf., Fig. 1). Journeying out from the Sun's core, an imaginary observer will first encounter temperatures of 15 MK, where energy is generated by nuclear reactions. Temperatures get progressively cooler *en route* to the photosphere, a mere 6000 K. But then something entirely unexpected happens: the temperature gradient reverses. The chromosphere's temperature steadily rises to 10,000 K, and going into the corona, the temperature jumps to 1 MK. Parts of the corona associated with sunspots get even hotter.

How does the Sun's radiation, leaving the 6000 K surface, could heat the outer atmosphere to much higher temperatures? This question became and remains one of the central questions in astrophysics (Dwivedi & Phillips 2003). For comprehensive reviews on topics concerning the Sun's interior till its exterior and the solar observing facilities, the reader is referred to 'Dynamic Sun' (Dwivedi 2003). The first clue to the million-degree hot corona emerged in the 1940s when B. Edlén identified that the 'green' coronal line, observed during total eclipses, was due to 13-times ionized iron. This led to the two most basic properties of the corona, namely, that it is rarefied gas and that its temperature is very high. The discovery of soft X-ray and ultraviolet emission in the post-World War II years provided further proof of the corona's high temperature.

2. Solar X-rays and ultraviolet emission

Spacecrafts, built by the U.S. and Soviet space agencies in the 1960s and 1970s, dedicated to solar observations added much to our knowledge of the Sun's atmosphere; notably the manned NASA Skylab mission of 1973–1974. Ultraviolet and X-ray telescopes onboard gave the first high-resolution images of the chromosphere and corona and the intermediate transition region. Images of active regions revealed a complex of

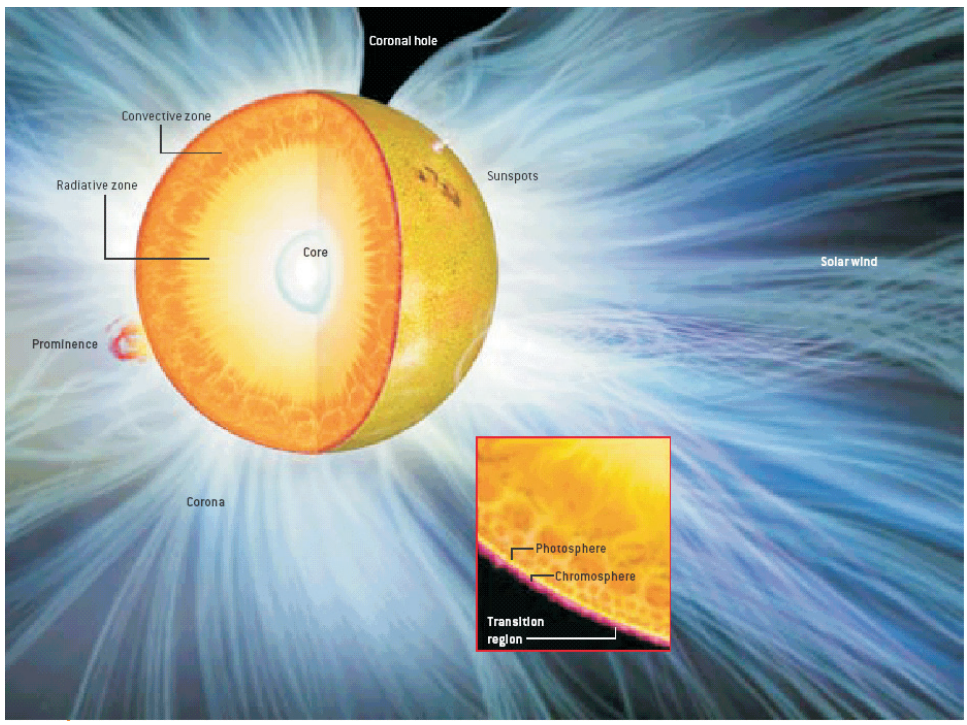

Figure 1. This figure gives a basic overview of the Sun's structure. The three major interior zones are the core (the innermost part of the Sun where energy is generated by nuclear reactions), the radiative zone (where energy travels outward by radiation through about 70% of the Sun), and the convection zone (in which convection circulates the Sun's energy to the surface). (Credit: Don Dixon.)

loops which varied greatly through their lifetimes, while ultraviolet images of the quiet Sun showed that the transition region and chromosphere followed the 'network' character previously known from Ca II K-line images. More recently, the spatial resolution of spacecraft instruments has steadily improved, nearly equal to what can be achieved with the ground-based solar telescopes (Mohan & Dwivedi 2001). Each major solar spacecraft since Skylab has offered a distinct improvement in resolution.

The ESA/NASA Solar and Heliospheric Observatory (SOHO), launched on December 2, 1995 into an orbit about the inner Lagrangian (L1) point, gives an uninterrupted view of the Sun (Dwivedi & Mohan 1997). There are several imaging instruments, sensitive from visible-light wavelengths to the extreme-ultraviolet. The Extreme-ultraviolet Imaging Telescope (EIT), for instance, uses normal incidence optics to get full-Sun images several times a day in the wavelengths of lines emitted by the coronal ions Fe IX/Fe X, Fe XII, Fe XV (emitted in the temperature range 600,000 K to 25,00,000 K) as well as the chromospheric He II 30.4 nm line. The Coronal Diagnostic Spectrometer (CDS) and the Solar Ultraviolet Measurements of Emitted Radiation (SUMER) are two spectrometers operating in the extreme-ultraviolet region, capable of obtaining temperatures, densities and other information from spectral line ratios. The Ultraviolet Coronagraph Spectrometer (UVCS) has been making spectroscopic observations of the extended corona from 1.25 to 10 solar radii from the Sun's centre,

determining empirical values for densities, velocity distributions and outflow velocities of hydrogen, electrons, and several minor ions. An intriguing observation with the UVCS has shown that particular ions, specifically highly ionized oxygen atoms, have temperatures in coronal holes, some 100 MK, that are much higher than those characterized by electrons and protons making up the bulk of the plasma (Kohl *et al.* 1997). There seems to be some directionality to the oxygen temperatures – they are higher perpendicular to the magnetic field lines than parallel to them, a result that is in agreement with interplanetary spacecraft sampling the particles making up the solar wind. The observation seems to call for high-frequency ion-cyclotron waves (Tu *et al.* 1998) that are produced lower down in the atmosphere as low-frequency waves but which through some cascade process end up at the observed frequencies. The excess broadening of coronal lines above the limb provides information on wave propagation in the solar wind. A striking difference in the width of line profiles observed on disk and in a polar coronal hole led to the discovery of the large velocity anisotropy, and consequently the possibility of the solar wind acceleration by ion-cyclotron resonance (Kohl *et al.* 1998).

The Transition Region and Coronal Explorer (TRACE) satellite went into a polar orbit around the Earth in 1998 (Handy *et al.* 1998). The spatial resolution is of order 1 arcsec (725 km), and there are wavelength bands covering the F IX, Fe XII, and Fe XV lines as well as the Ly-alpha line at 121.6 nm. Its ultraviolet telescope has obtained images containing a tremendous amount of small and varying features, for instance, active region loops are revealed to be only a few hundred kilometers wide, almost thread-like compared to their huge lengths. Their constant flickering and jouncing hint at the corona's heating mechanism. There is a clear relation of these loops and the larger arches of the general corona to the magnetic field measured in the photospheric layer. The crucial role of this magnetic field has been realized only during the past decade. The fields dictate the transport of energy between the surface of the Sun and the corona. The loops, arches and holes appear to trace out the Sun's magnetic field. The latest in the fleet of spacecraft dedicated to viewing the Sun is the Reuven Ramaty High Energy Solar Spectroscopic Imager (RHESSI), launched in 2002, which provides images and spectra in hard X-rays (wavelengths less than about 4 nm). RHESSI's observations of tiny microflares may provide clues to the coronal heating mechanism (Lin *et al.* 2002).

We can directly measure physical parameters such as electron density, temperature, flow speeds, etc. in the corona from emission line diagnostics. However, we cannot directly measure magnetic field strength, resistivity, viscosity, turbulence, waves, etc. New powerful tools of coronal seismology have enabled the detection of MHD waves by TRACE and EIT, spectroscopic measurements of line-widths by SUMER and CDS, ion and electron temperature anisotropy measurements with UVCS, and now microflares by RHESSI.

3. Coronal heating

The corona is a magnetically dominated environment consisting of a variety of plasma structures including X-ray bright points, coronal holes and coronal loops or arches (cf., Fig. 2). There is strong but indirect evidence to suggest that corona is heated by magnetic fields. One vital piece of information that we are still unable to measure is the corona's magnetic field strength. We can measure with considerable accuracy,

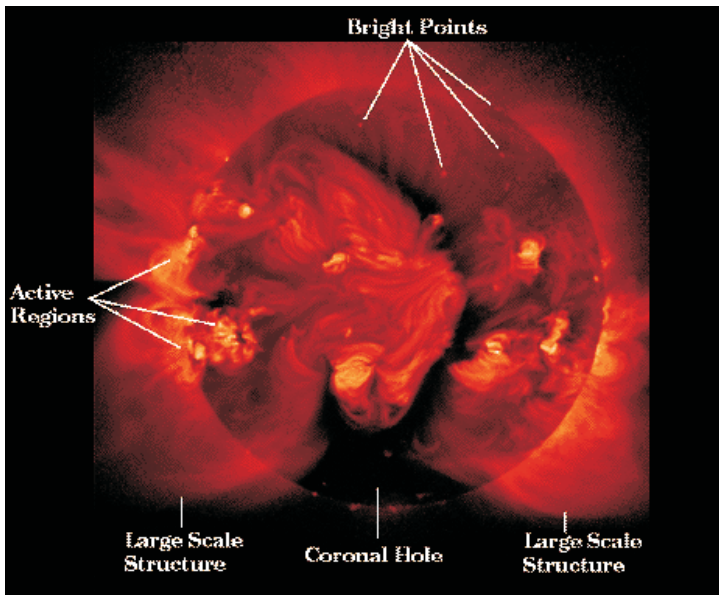

Figure 2. The X-ray Sun showing variety of plasma structures. (Credit: SXT/Yohkoh.)

the photospheric magnetic field using magnetographs that work on the Zeeman effect. Although, eventually, infrared measurements may give important information, practically the only way at present in which the coronal field can be deduced is through particular assumption: either that there are no currents flowing in the plasma (current-free), i.e., $\nabla \times \mathbf{B} = 0$, or that currents, if they exist, run parallel to magnetic field lines (force-free), i.e., $\mathbf{J} \times \mathbf{B} = 0$. These predict that the magnetic field of the corona generally has a strength of about 10 gauss. In active regions, the field may reach 100 gauss. It is to be noted, however, that vibrating magnetic structures in the solar atmosphere are opening up a new way to study the Sun. By fitting the observed oscillations from the TRACE spacecraft with MHD wave theory, Nakariakov & Ofman (2001) have determined the magnetic field strength in a coronal loop to be of about 13 gauss. The photospheric field in active region corona is more complex than in quiet regions and also the active region corona is appreciably hotter than in quiet regions. Thus there seems to be a relation between magnetic field strength, its complexity and heating.

A considerable problem with magnetic field heating is the fact that it requires the diffusion, and therefore reconnection, of magnetic field which implies a resistive plasma. However, the coronal plasma is, on the contrary, highly conducting. Using the induction equation of magnetohydrodynamics (MHD), we find that the diffusion time for a magnetic field is extremely long. If the characteristic distance over which diffusion occurs is as short as a few meters, then the diffusion time is a few seconds. In other words, the magnetic Reynolds number R_m, which measures how tied the magnetic field is to the plasma, is typically 10^{12} for the corona, indicating that the field is completely 'frozen in' to the plasma. However, reconnection requires R_m to be very small, much less than one. Thus, only if the length scales are very small (a few meters), can one achieve magnetic reconnection. Very small length scales do occur in the region of neutral points or current sheets, where there are steep magnetic field gradients which give

rise to large currents. It is thought, then, that such geometries are important for coronal heating if this is by very small energy releases, known as nanoflares. Some 10^{16} J are released in a nanoflare, which is 10^{-9} of a large solar flare. Many energy releases like this occuring all over the Sun, quiet as well as active regions, could account for heating of the corona. However, it is doubtful whether this mechanism would apply to coronal hole regions where the field lines are open to interplanetary space (for more details, see Phillips & Dwivedi 2003).

The above reasoning applies equally to the competing wave heating hypothesis of coronal heating, in which MHD waves generated by photospheric motions (e.g., granular or supergranular convection motions) are damped in the corona. In this case, we need conditions such that the magnetic field changes occur in a shorter time than, say the Alfvén wave transit time across a closed structure like an active region or quiet Sun loop. The waves, generated by turbulent motions in the convection zone or at the photosphere, may be surface waves, or body waves which are guided along the loops and are trapped. Theoretical work shows that short-period fast-mode and slow-mode waves (periods less than 10 s) could be responsible for heating (Porter *et al.* 1994) since the damping rates are high enough only for them. It is possible that (and would certainly be simpler) if X-ray bright points, coronal holes and the different types of coronal loops (see Fig. 2) are heated by the same mechanism, but it is also possible that they are heated by different mechanisms. The debate on coronal heating centres on whether the field energy is dissipated via numerous small magnetic reconnections ('nanoflares'), or damping of MHD waves which emerge from the interior and pass through the Sun's surface layers to the corona.

The over-riding problem for both theories is the way reconnections or MHD waves manage to dissipate current energy into heat energy in view of the fact that the corona is highly conducting. TRACE observations and analysis of damped coronal magnetic loop oscillations provide evidence that the resistivity of the corona is not in fact as low as it would seem classically (Nakariakov *et al.* 1999). But rather, there are anomalous processes in which heat dissipation occurs via particle-wave interactions instead of particle–particle collisions. If the resistivity is enhanced (or the resistivity and the viscosity are enhanced), then it would support the dissipation of waves and magnetic reconnection mechanisms for coronal heating.

Although the weight of observational evidence generally points to a nanoflare mechanism for providing the bulk of coronal heating, MHD waves probably contribute significantly. It is, for example, unlikely that nanoflares could have much effect in coronal holes. In these regions, the field lines open out into space rather than loop back to the Sun, so a reconnection would accelerate plasma rather than heat it. Yet the corona in holes is still hot. Astronomers have therefore scanned coronal holes as well as closed field regions for signatures of wave motions, which may include periodic fluctuations in brightness. The difficulty is that the MHD waves involved in heating probably have very short periods, just a few seconds. At present, spacecraft imaging is too sluggish to capture them. For this reason ground-based instruments operating during total eclipses are still important.

4. Wave activity

Hassler *et al.* (1990) carried out rocket-borne experiments to observe off-limb linewidth profile of Mg X 609 and 625 Å and reported the increasing linewidth with altitude

(up to 70,000 km). This observation provided the signature of outward propagating undamped Alfvén waves. SUMER and CDS spectrometers on SOHO recorded several line profiles and found the broadening of emission lines. These results are consistent with outward propagation of undamped Alfvén waves travelling through regions of decreasing density (Erdélyi *et al.* 1998). Harrison *et al.* (2002) reported the narrowing of the Mg X 62.50 nm line with height in the quiet near-equatorial solar corona, and concluded that this narrowing is a likely evidence of dissipation of Alfvén waves in closed field-line regions. Similarly, a significant change in slope of the linewidth as a function of height was seen in polar coronal holes by O'Shea *et al.* (2003) at an altitude of $\approx$ 65 Mm. These results obtained with the CDS spectrometer, if confirmed, could be crucial in understanding the coronal heating mechanisms. Due to the broad instrumental profile, the CDS instrument can only study line-width variations and cannot provide measurements of the linewidth itself, and, hence, of the effective ion temperature. Since the latter quantity is critical in constraining theoretical models of coronal heating and solar-wind acceleration, for instance, through the dissipation of high-frequency waves generated by chromospheric reconnection, Wilhelm *et al.* (2004) studied the problem further by analysing data recorded with the SUMER spectrograph in the Mg X doublet together with other neighbouring lines in both the quiet equatorial corona and in a polar coronal hole. Due to the high spectral resolution of SUMER, they were able to obtain profiles of both Mg X emission lines and measure their widths and variations as a function of height. Their work showed that linewidths of both components of the Mg X doublet measured by SUMER monotonically increase in the low corona in equatorial regions in altitude ranges for which scattered radiation from the disk does not play a major role. They did not find any evidence for a narrowing of the emission lines above 50 Mm. The same statement applies for a coronal hole, but they could not exclude the possibility of a constant width above 80 Mm (cf., Fig. 3).

While there have been reports of emission-line broadening with altitude, using SUMER, the CDS observations presented by Harrison *et al.* (2002) appeared to show emission-line narrowing. In order to resolve the apparent discrepancies, a joint CDS/SUMER observational sequence was successfully executed during the SOHO/MEDOC campaign in November and December 2003. The joint measurements were performed near the east limb (cf., Wilhelm *et al.* 2005). The pointing locations of the spectrometers are shown in Figs. 4(a) and 4(b) superimposed on He II and Fe XII solar images taken by EIT (Wilhelm *et al.* 2005). In the western corona, SUMER made additional exposures with a similar observational sequence from 13:02 to 15:06 UTC. Since the corona was very hot there, the slit positions are shown together with the Fe XII and Fe XV windows of EIT in Fig. 4(c) and 4(d).

The relative widths of the spectral lines observed by SUMER are shown in Fig. 5, separately for the eastern and western FOVs. In cases for which more than one observation was available, mean values have been shown. The range of $\nu_{1/e}$ extends from 35 km s^{-1} to 49 km s^{-1} in the relatively quiet eastern corona, and from 33 km s^{-1} to 48 km s^{-1} in the active western corona. No significant differences could be noticed within the uncertainty margins. The Mg X and Ca X lines show slight increases with height in the east, but are rather constant in the west. The Fe XII line is a little narrower in the west. Of particular interest was that the lines of Ca XIII and Fe XVIII were seen in the west, where they could be compared with the Ca X and Fe XII lines along the same LOS. In the relatively quiet equatorial corona above a small prominence, Wilhelm *et al.* (2005) found none or very slight increase of the linewidths of coronal emission lines

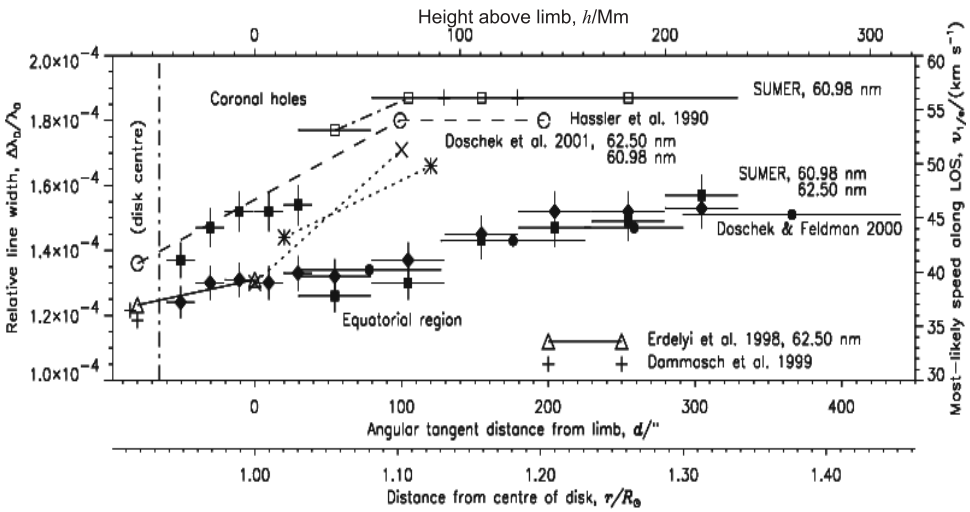

Figure 3. Relative linewidth variations as a function of radial distance from the Sun. Literature data and results obtained in this work (annotated 'SUMER') are compiled for the Mg X doublet in equatorial and coronal-hole regions. A classification of the Hassler *et al.* observations, of which only three typical values are shown, is not defined in their 1990 paper. An approximate scale of 715 km has been used for both the SOHO observations and those from the Earth. Integration intervals and the SUMER uncertainty margins are marked by horizontal and vertical bars. Related data points are in some cases connected by lines of various styles. These are meant to improve the orientation for the reader, but not as physical interpolations, in particular, for those points representative of centre-of-disk values displayed here near $-80''$ (from Wilhelm *et al.* 2004).

with altitude from measurements both with CDS and SUMER. Taking the combined uncertainty margins into account, the relative variations for Mg X were considered to be consistent, although the absolute widths could not be compared given the different instrumental spectral transfer functions. The SUMER observations indicated even less line-width variations with height in the more active corona. Singh *et al.* (2003) found height variations of line profiles in the visible light that depended on the formation temperatures of the lines. So, the solar conditions appear to have a direct influence on the line-width variations with height. Whether this dependence can account for the past apparent discrepancies cannot be decided unambiguously with the information available. More observations for different coronal activity levels are needed for this task. However, this joint study concluded that CDS and SUMER relative line-width measurements did not lead to inconsistencies if the same solar region was under study.

5. Coronal holes and the solar wind

Observations from the Skylab firmly established that the high-speed solar wind originates in coronal holes which are well-defined regions of strongly-reduced ultraviolet and X-ray emissions (Zirker 1977). More recent data from Ulysses show the importance of the polar coronal holes, particularly at times near the solar minimum, when dipole field dominates the magnetic field configuration of the Sun. The mechanism for accelerating the wind to the high values observed, of the order of 800 km s^{-1}, is not yet fully understood. The Parker model is based on a thermally-driven wind. To

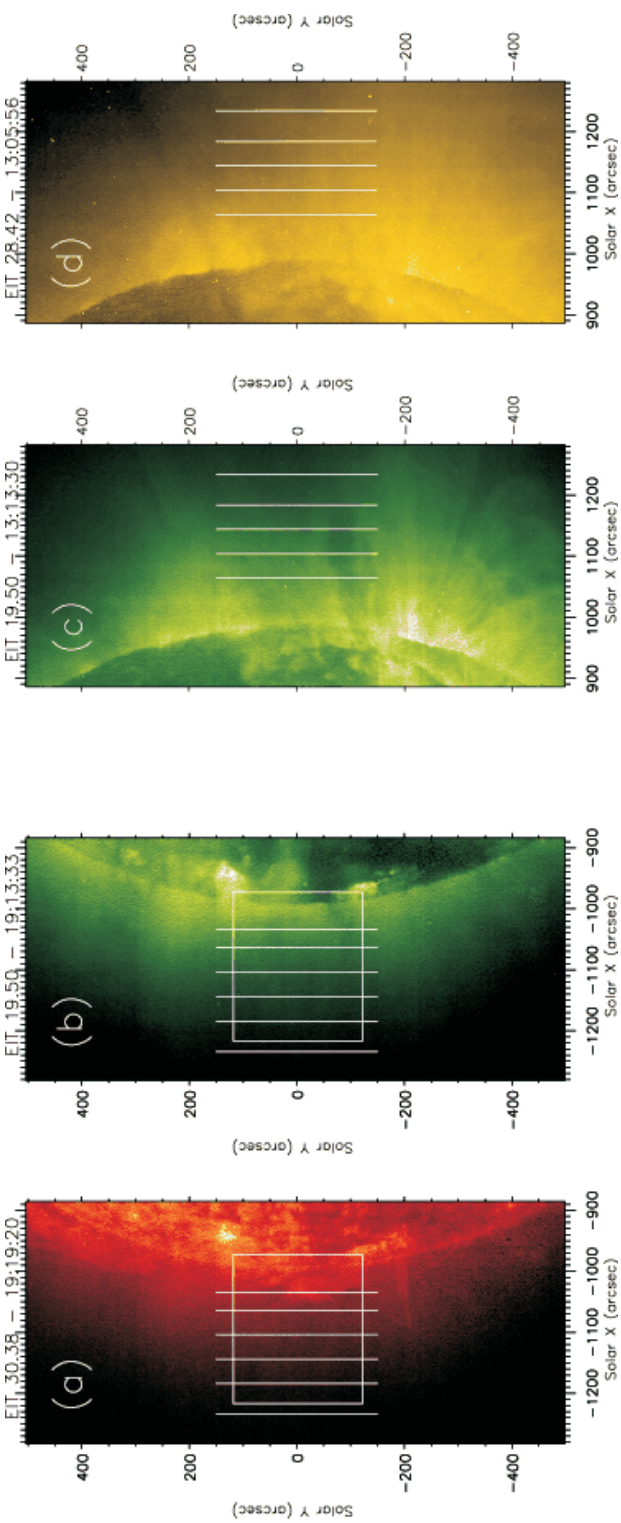

Figure 4. Positions of the CDS FOVs (rectangles) and the SUMER slit pointing locations in relation to He II, Fe XII and Fe XV solar images of 4 December 2003 (courtesy of the EIT consortium). Joint observations were obtained in the eastern corona. At low altitudes, a prominence caused a slight disturbance there. **(a)** He II spectral window; and **(b)** Fe XII window near the east limb; **(c)** Fe XII window; and **(d)** Fe XV window near the west limb (from Wilhelm *et al.* 2005).

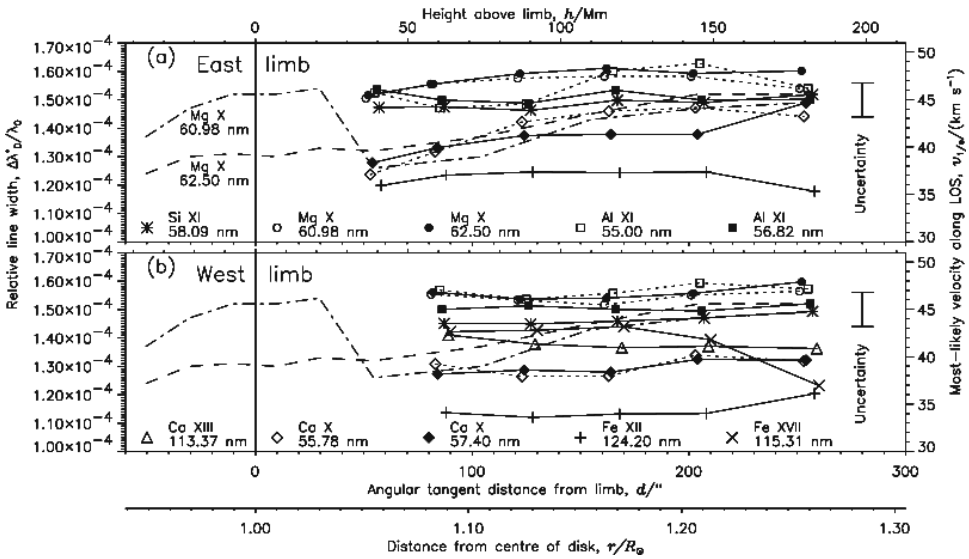

Figure 5. Summary of the SUMER linewidth measurements in terms of the relative linewidth, $\Delta\lambda_D^*/\lambda_D$, of the various ions, as well as their most-likely velocity along the LOS, $v_{1/e}$, as a function of distance from the limb. **(a)** Measurements above the east limb; **(b)** above the west limb. The dashed and dash-dotted lines indicate the Mg X observations of SUMER in November 1996. The increase of the width of the 60.98 nm line near the limb is caused by blends of O III and O IV transition-region lines (cf. Wilhelm *et al.* 2004). Near the centre of the solar disk a value of $\Delta\lambda_D^*/\lambda_D \approx 1.2 \times 10^{-4}$ was observed for Mg X (Erdélyi *et al.* 1998). At each slit position, an altitude range of $\approx 10''$ was covered. In the interest of clarity, we spread the plot symbols of the various spectral lines over this range (from Wilhelm *et al.* 2005).

reach such high velocities, temperatures of the order 3 to 4 MK would be required near the base of the corona. However, other processes are available for acceleration of the wind, for example, the direct transfer of momentum from MHD waves, with or without dissipation. This process results from the decrease of momentum of the waves as they enter less dense regions, coupled with the need to conserve momentum of the total system. If this transfer predominates, it may not be necessary to invoke very high coronal temperatures at the base of the corona.

Prior to the SOHO mission, there was very little information available on the density and temperature structure in coronal holes. Data from Skylab was limited, due to the very low intensities in holes and poor spectral resolution, leading to many line blends. High-resolution ultraviolet observations from instruments on SOHO spacecraft provided the opportunity to infer the density and temperature profile (see Fig. 6a) in coronal holes (Wilhelm *et al.* 1998). Comparing the electron temperatures with ion temperatures, it was concluded that ions are extremely hot and the electrons are relatively cool. Using the CDS and SUMER instruments on the SOHO spacecraft, electron temperatures were measured as a function of height above the limb in a coronal hole. Observations of two lines from the same ion, O VI 1032 Å from SUMER and O VI 173 Å from CDS, were made to determine temperature gradient in a coronal hole (David *et al.* 1998). This way temperature of around 0.8 MK close to the limb was deduced, rising to a maximum of less than 1 MK at 1.15 $R_\odot$ (see Fig. 6b), then falling

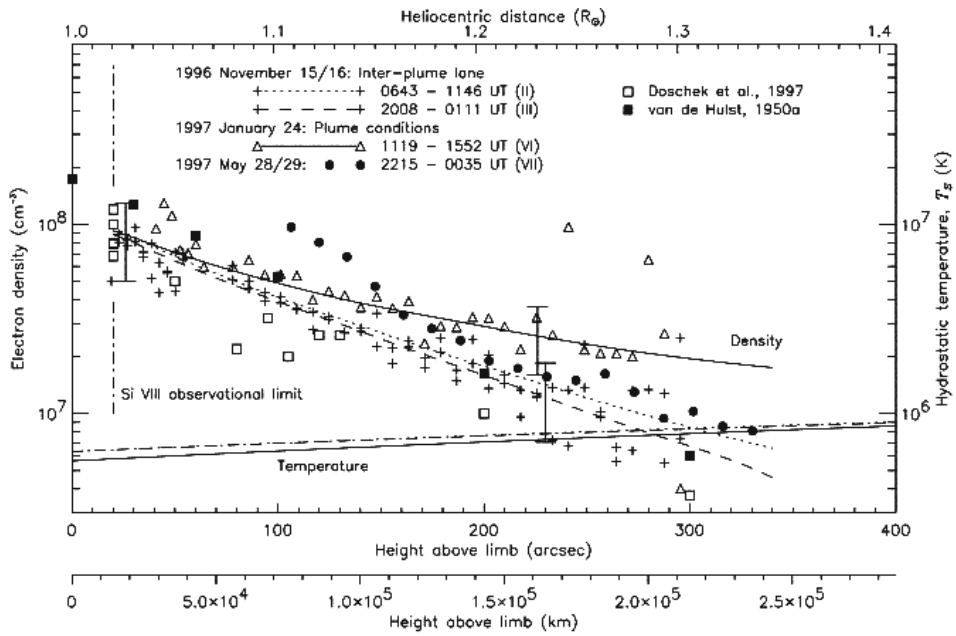

Figure 6(a). Electron densities derived from Si VIII line ratios and a comparison with data in the literature. The hydrostatic temperature, TS, used for the fits of the line Si VIII (1445 Å) is plotted in the lower portion of the diagram, with a scale on the right-hand side. The points labeled '1997 May 28/29' are obtained from the ratios observed west of the polar plume assembly in a very dark region of the corona. The error bars indicate a density variation resulting from a $\pm 30\%$ uncertainty in the line ratio determination. Note that there is a small (3%) seasonal variation between the angular and the spatial scales for different data sets (from Wilhelm *et al.* 1998).

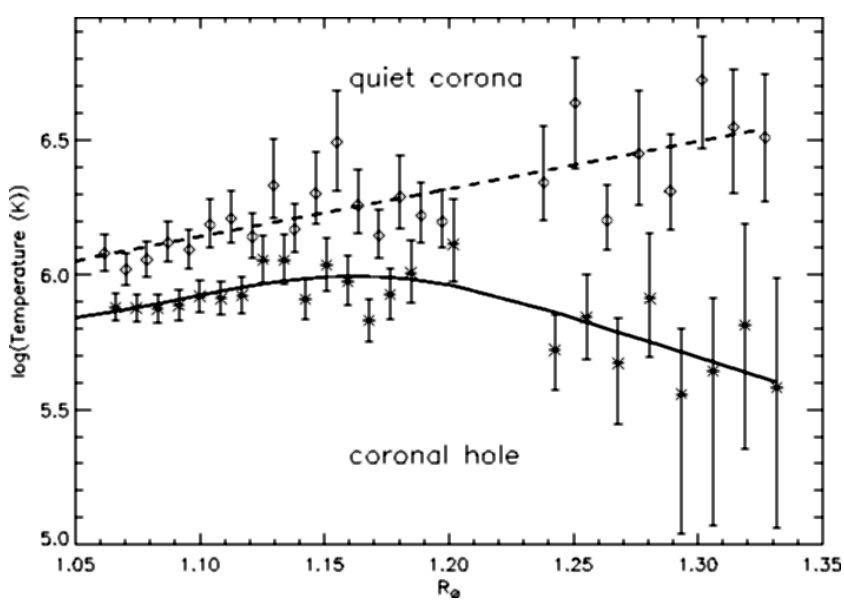

Figure 6(b). Temperature gradient measurement in the quiet corona (equatorial west limb) and the north polar coronal hole (from David *et al.* 1998).

to around 0.4 MK at 1.3 $R_{\odot}$. These observations preclude the existence of temperatures over 1 MK at any height near the centre of a coronal hole. Wind acceleration by temperature effects is, therefore, inadequate as an explanation of the high-speed solar wind, and it becomes essential to look for other effects, involving the momentum and the energy of Alfvén waves.

That the solar wind is emanating from coronal holes (open magnetic field regions in the corona) has been widely accepted since the Skylab era. But there was little additional direct observational evidence to support this view. Hassler *et al.* (1999) found the Ne VIII emission blue shifted in the north polar coronal hole along the magnetic network boundary interfaces compared to the average quiet-Sun flow (cf., Fig. 7). These Ne VIII observations reveal the first two-dimensional coronal images showing velocity structure in a coronal hole, and provide strong evidence that coronal holes are indeed the source of the fast solar wind.

Tu *et al.* (2005) have now successfully identified the magnetic structures in the solar corona where the fast solar wind originates. Using images and Doppler maps from the SUMER spectrograph and magnetograms from the MDI instrument on the SOHO

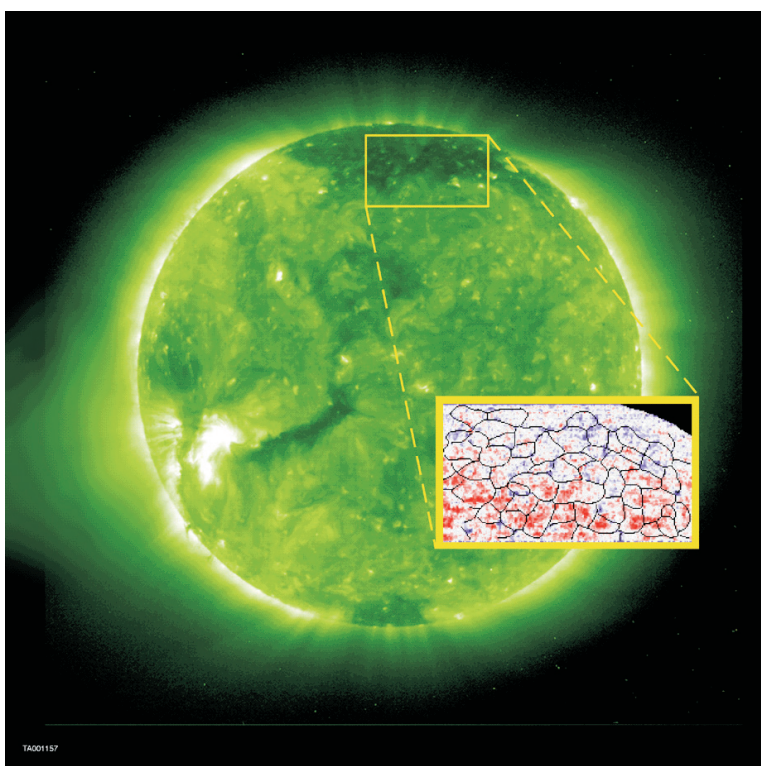

Figure 7. The solar corona and polar coronal holes observed from EIT and SUMER instruments on SOHO. The 'zoomed-in' or 'close-up' region in the image shows a Doppler velocity map of million degree gas at the base of the corona where the solar wind originates. Blue represents blue shifts or outflows and red represents red shifts or downflows. The blue regions are inside a coronal hole or open magnetic field region, where the high-speed solar wind is accelerated. Superposed are the edges of 'honeycomb'-shaped patterns of magnetic fields at the surface of the Sun, where the strongest flows (dark blue) occur (Credit: Don Hassler and SUMER-EIT/SOHO).

spacecraft, they have reported the solar wind flowing from funnel-shaped magnetic fields which are anchored in the lanes of the magnetic network near the surface of the Sun. This landmark research leads to a better understanding of the magnetic nature of the solar wind source region. The heavy ions in the coronal source regions emit radiation at certain ultraviolet wavelengths. When they flow towards Earth, the wavelengths of the ultraviolet emission become shorter which can be used to identify the beginning of the solar wind outflow.

Previously it was believed that the fast solar wind originates on any given open field line in the ionization layer of the hydrogen atom slightly above the photosphere. However, the low Doppler shift of an emission line from carbon ions shows that bulk outflow has not yet occurred at a height of 5000 km. The solar wind plasma is now considered to be supplied by plasma stemming from the many small magnetic loops, with only a few thousand kilometers in height, crowding the funnel. Through magnetic reconnection plasma is fed from all the sides to the funnel, where it may be accelerated and finally form the solar wind. The fast solar wind starts to flow out from the top of funnels in coronal holes with a flow speed of about 10 km s^{-1}. This outflow is seen as large patches in Doppler blue shift (hatched areas in the image) of a spectral line emitted by Ne^{+7} ions at a temperature of 600,000 K, which can be used as a good tracer for the hot plasma flow (see Fig. 8). Through a comparison with the magnetic

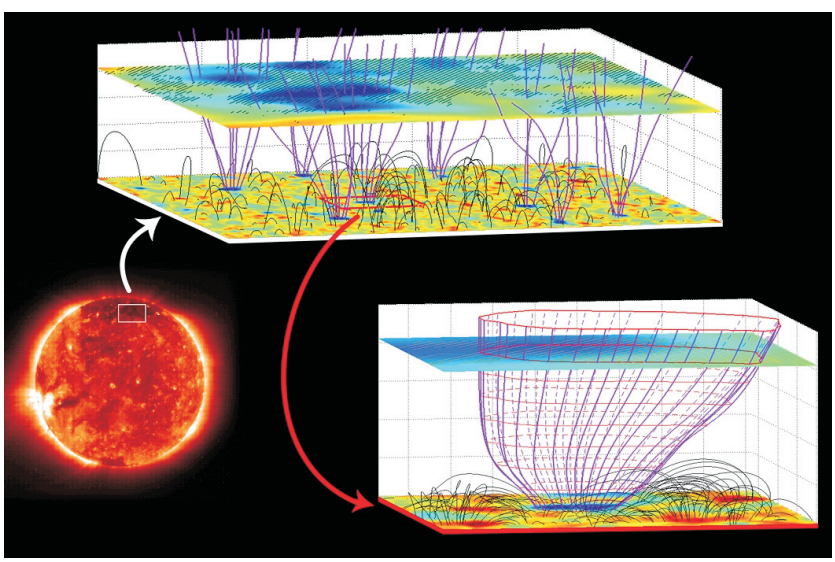

Figure 8. This picture was constructed from measurements which were made on September 21, 1996 on SOHO with the SUMER for Doppler spectroscopy of the coronal plasma, with the MDI for magnetograms of the Sun's surface, and the EIT for the context image of the Sun. The figure illustrates location and geometry of three-dimensional magnetic field structures in the solar atmosphere. The magenta coloured curves illustrate open field lines, and the dark gray solid arches show closed ones. In the lower plane, the magnetic field vertical component obtained at the photosphere by MDI is shown. In the upper plane, inserted at 20,600 km, the Ne VIII Doppler shift is compared with the model field. The shaded area indicates where the outflow speed of highly charged neon ions is larger than 7 km s^{-1}. The scale of the figure is significantly stretched in the vertical direction. The smaller figure in the lower right corner shows a single magnetic funnel, with the same scale in both vertical and horizontal directions (Tu *et al.* 2005) (Credit: SUMER, ESA/NASA).

field, as extrapolated from the photosphere by means of the MDI magnetic data, it has been found that the blue-shift pattern of this line correlates best with the open field structures at 20,000 km (Tu *et al.* 2005).

6. Concluding remarks

A large amount of information concerning the physics of the Sun's hot atmosphere has been made available in recent years from highly successful spacecraft and from ground-based instruments. We have made tremendous progress in pinpointing the processes that maintain the Sun's hot corona and accelerate the solar wind as well as the identification of its source region. And the search goes on.

Acknowledgements

This work is supported by the Indian Space Research Organization (ISRO) under its RESPOND programme. The author is indebted to an anonymous referee for helpful comments.

References

David, C., Gabriel, A. H., Bely-Dubau, F., Fludra, A., Lemaire, P., Wilhelm, K. 1998, *Astron. Astrophys.*, **336**, L90.
Dwivedi, B. N., Mohan, A. 1997, *Curr. Sci.*, **72**, 437.
Dwivedi, B. N., Phillips, K. J. H. 2003 *The Paradox of the Sun's Hot Corona*, In: The Scientific American special edition "New Light on the Solar System" (updated from the Scientific American June 2001 issue) pp. 4–11.
Dwivedi, B. N. (ed.) 2003 *Dynamic Sun*, Cambridge University Press.
Erdélyi, R., Doyle, J. G., Perez, M. E., Wilhelm, K. 1998, *Astron. Astrophys.*, **337**, 287.
Handy, B. N., Bruner, M. E., Tarbell, T. D. *et al.* 1998, *Solar Phys.*, **183**, 29.
Harrison, R. A., Hood, A. W., Pike, C. D. 2002, *Astron. Astrophys.*, **392**, 319.
Hassler, D. M., Rottman, G. J., Shoub, E. C., Holzer, T. E. 1990, *Astrophys. J.* **348**, L77.
Hassler, D. M., Dammasch, I. E., Lemaire, P. *et al.* 1999, *Science*, **283**, 810.
Kohl, J. L., Noci, G., Antonucci, E. *et al.* 1997, *Solar Phys.*, **175**, 613.
Kohl, J. L., Noci, G., Antonucci, E. *et al.* 1998, *Astrophys. J. Lett.*, **501**, L127.
Lin, R. P., Dennis, B. R., Hurford, G. J. *et al.* 2002, *Solar Phys.*, **210**, 3.
Mohan, A., Dwivedi, B. N. 2001, *Curr. Sci.*, **81**, 349.
Nakariakov, V. M., Ofman, L. 2001, *Astron. Astrophys.*, **372**, L53.
Nakariakov, V. M., Ofman, L., DeLucca, E. E., Roberts, B., Davila, J. M. 1999, *Science*, **285**, 862.
O'Shea, E., Banerjee, D., Poedts, S. 2003, *Astron. Astrophys.*, **400**, 1065.
Phillips, K. J. H. P., Dwivedi, B. N. 2003, In: *Dynamic Sun* (ed.) B. N. Dwivedi, Cambridge University Press, pp. 335–352.
Porter, L. J., Porter, J. A., Sturrock, P. A. 1994, *Astrophys. J.*, **435**, 482.
Singh, J., Ichimoto, K., Sakurai *et al.* 2003, *Astrophys. J.*, **585**, 516.
Tu, C.-Y., Marsch, W., Wilhelm, K., Curdt, W. 1998, *Astrophys. J.*, **503**, 475.
Tu, C.-Y., Zhou, C., Marsch, E. *et al.* 2005, *Science*, **308**, 519.
Wilhelm, K., Marsch, E., Dwivedi, B. N., Hassler, D. M., Lemaire, P., Gabriel, A. H., Huber, M. C. E.1998, *Astrophys. J.*, **500**, 1023.
Wilhelm, K., Dwivedi, B. N., Teriaca, L. 2004, *Astron. Astrophys.*, **415**, 1133.
Wilhelm, K., Fludra, A., Teriaca, L., Harrison, R. A., Dwivedi, B. N., Pike, C. D. 2005, *Astron. Astrophys.*, **435**, 733.
Zirker, J. B. (ed.) 1977, *Coronal Holes and High Speed Solar Wind Streams*, Colorado Associated Univ. Press, Boulder.